Multielectronic excitations near the K edge of argon

Moshe Deutsch and Nissan Maskil
Physics Department, Bar-Ilan University, Ramat-Gan 52900, Israel

Wolfgang Drube
Hamburger Synchrotronstrahlungslabor at Deutsches Elektronensynchrotron, D-2000 Hamburg 52, Germany
(Received 3 April 1992)

High-resolution x-ray photoabsorption measurements on Ar near its K edge are reported. A number of new two-electron KM features were detected. The three-electron KM^2 and the two-electron KL spectra were measured. The previously unresolved three-electron KM^2 and the two-electron KL spectra were clearly resolved in this study. Identification of spectral features is discussed based on our Hartree-Fock and published Dirac-Fock [Dyall, J. Phys. B **16**, 3137 (1983); Dyall and LaVilla, Phys. Rev. A **34**, 5123 (1986)] energy-level calculations.

PACS number(s): 32.80.Hd, 32.30.Rj

Multielectron processes in atoms depend sensitively on intra-atomic correlations and the dynamics of the excitation. They can provide, therefore, an insight into the electronic structure and the excitation process which goes beyond prevailing single-electron fixed-potential models. X-ray near-edge photoabsorption measurements in noble gases, which are free from extended x-ray-absorption fine-structure (EXAFS) interference and probe the energies and cross sections directly, are particularly well suited for these studies. The near-K-edge spectra of neon [1], argon [2], krypton [3], and xenon [4] were measured with high resolution, showing a rich array of two-electron ($2e$) and even some three-electron ($3e$) excitations. In particular, the very detailed measurements of Deslattes *et al.* [2] on Ar were repeatedly used to test models for the excitation dynamics and the importance of effects, such as post-collisional interaction, exchange, ground-, and final-state correlations and relaxation [5–8]. However, sharp features involving $2e$ $\underline{1s3s}$ and $3e$ $\underline{1s3ll'}$ states could not be resolved in those synchrotron-radiation measurements (underline denotes hole states). Furthermore, no $\underline{1s2l}$ features were reported to date for Ar, although such features were detected in Ne [1] and Kr [3]. We report here high-resolution measurements of the photoabsorption spectrum of Ar in the KM and KL regions. A number of previously unresolved $\underline{1s3p}$ and $\underline{1s3s}$ features were detected, and the $3e$ KM^2 and $2e$ KL features were resolved. Tentative identification of these, based on our Hartree-Fock (HF) energy-only and published [9, 7] Dirac-Fock (DF) calculations, is also presented.

The measurements were done at the EXAFS II mirror-focused beamline at HASYLAB in a standard transmission EXAFS configuration, using an UHV-compatible double-crystal Si(111) monochromator. Harmonics were effectively eliminated by detuning the monochromator crystals using a stabilization feedback control [10]. The flux at the sample was $\sim 10^{10}$ photons/sec and the energy resolution $\Delta E \approx 0.9$ eV. Reference scans without sample were done to obtain absolute cross sections. Incident beam stability and measurements statistics were high enough to allow confident detection of features as small as 0.02% of the K edge. The energy scale was established using the resonance line at [11] $E_{1s\rightarrow 4p}=3203.54$ eV.

The energy levels were calculated using the nonrelativistic HF code HF86 of Fischer [12]. As per the usual change in the self-consistent-field (ΔSCF) scheme, the final-state energies were calculated each in a separate, single-configuration (SC) run and the resultant average energies subtracted from that of the $\underline{1s}$ configuration, calculated in the same manner. While this procedure accounts for the relaxation of the excited atom, it does not account for initial- and final-state correlation effects which were also demonstrated to be very important for two-electron transitions in the recent multiconfiguration HF studies of Saha [5] and Cooper [6]. Although calculated energies are less sensitive to the inclusion of such effects than cross sections, it is clear that our single-configuration HF, energy-only calculations should be regarded as tentative. A definite identification will require a detailed multiconfigurational energy and cross-section

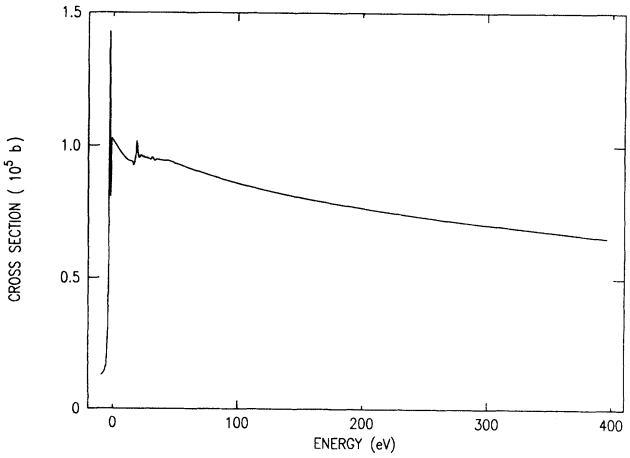

FIG. 1. Near-K-edge photoabsorption spectrum of Ar. Zero energy is at the edge, $E_K=3206.26$ eV.

calculation along the lines of Saha [5] and Cooper [6], taking the effects mentioned above into consideration through the configuration interaction (CI) procedure.

The measured cross section σ is given in Fig. 1, with zero energy at the edge [11] E_K=3206.26 eV. It is a few percent lower than, but close to, that of Deslattes *et al.* [2]. The uncertainty in the absolute value is ~6%. The KM multielectronic features at $E \geq 15$ eV are shown on an expanded scale in Fig. 2, along with the calculated HF energies. The alphabetic feature designation is identical to that of Deslattes *et al.* [2]. Additional features, including the new ones, are numbered A1, B1, etc. The proposed feature identification is given in Table I, along with the calculated HF energies. As the most prominent features were discussed by several authors [2, 7, 6, 5] we will concentrate mostly on the newer features in the data.

The $1s3p$ *region.* The shoulders A1, B1, and B2 are well aligned with $1s3p4s3d, 4s$, and $3d$, respectively. As they are populated by a dipole conjugate (CSU) rather than a monopole shake-up process (SU), their cross sections are small. Peaks C and C1 are well aligned with $1s3p4p$ whose full spin-orbit splitting (SOS), shown in Fig. 3, is 1.3 eV. D2, shown in Fig. 4 after subtracting a straight line fitted to the data below the feature, is mostly due to the single-ion edge $1s3p6p$, with contributions from $6p^2$ and the CSU $5d, 6s$, and $6s^2$. Its width is commensurate with the ~0.8 eV SOS calculated by Dyall [9]. A reliable separation of the measured cross section into the contributions of individual transitions is an extremely complicated task requiring accurate cross-section and energy-level calculations. We will resort, therefore, to the admittedly somewhat arbitrary but previously employed [3, 4, 13] procedure of fitting a straight line just below the relevant feature, and calculating the ratio of the feature's height above this line to that of the K-edge jump, to obtain the "measured" relative cross section. Here, the measured relative cross section, ~0.05%, is much smaller than the calculated 2.5%, which, however, should be treated with caution as pointed out by Dyall

TABLE I. Feature identification for multielectronic excitation in argon. Labels refer to Figs. 2–7.

Label	Present	HF	Deslattes[a]	Dyall[b]
A	$1s3p4s^2$	15.2	$4s^2$	$4s^2$
A1	$4s3d$	17.2		$4s3d$
B	$4p^2$	19.2	$4p^2, 4s3d$	$4p^2$
	$4d^2$	20.0		
B1	$4s$	20.0		
B2	$3d$	21.6		
C	$(^3P)4p$	22.4	$4p$	$4p5p$
C1	$(^1P)4p$	23.1		
	$5s^2$	23.5		
D	$5p^2$	24.8	$5s, 5p$	$5p^2$
	$5s$	25.7		
D1	$5p$	26.6		
	$4d$	26.2		
D2	$6p^2$	27.1		
	$6p$	28.2		
E	$1s3p$	30.8	$1s3p$	$1s3p$
	$1s3s4s4p$	35.4	$1s3s4s4p$	$1s3s4s4p$
F	$1s3s(^3S)4s4p$	35.4	$4s4p$	
F1	$(^1S)4s4p$	36.7		
F2	$4s$	39.7	$4s$	$5s4p$
	$5s4p$	40.5		
F3	$3d$	41.0		
G	$5s5p$	43.7		
	$4p$	42.4		
G1	$5s$	45.5		
	$4d$	46.0		
G2	$6s$	47.6		
	$5d$	47.6		
H	$1s3s$	50.6	$1s3s$	$1s3p^24p^3$
			$1s3p^24p^2$	$4s^24p$
H1	$1s3p^24p^2(^4P)$	51.7[c]		
H2	$4p^2(^2D, S)$	51.7[c]		
H3	$4p(^{4,2}P)$	61.2[c]		
H4	$4p(^2D, S)$	61.2[c]		
H5	$1s3p^2$	76.5[c]		
I1,2	$1s2p(^3P)4p^2$	293.3		
	$(^3P)4p$	296.9		
J1,2	$(^1P)4p^2$	304.4		
	$(^1P)4p$	308.0		
	$5p^2$	302.0		
K1	$1s2p(^3P)$	305.3		

[a]Reference [2].

[b]Reference [7].

[c]Average energy. Spin-orbit splitting is ~6 eV.

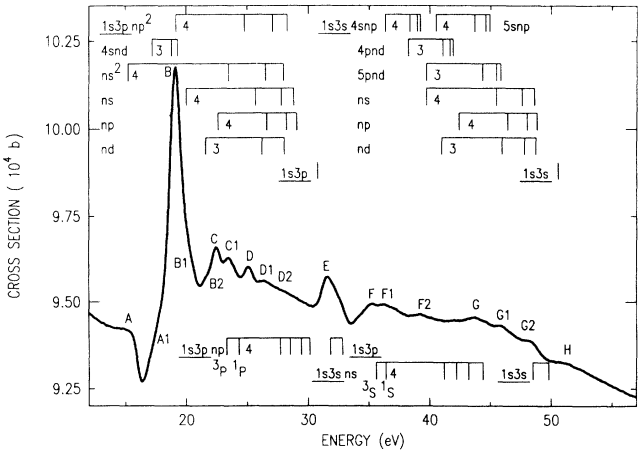

FIG. 2. Expanded view of the KM double-excitation region. The energy levels above the curve are the present HF ones, while those below it are DF values from Ref. [7].

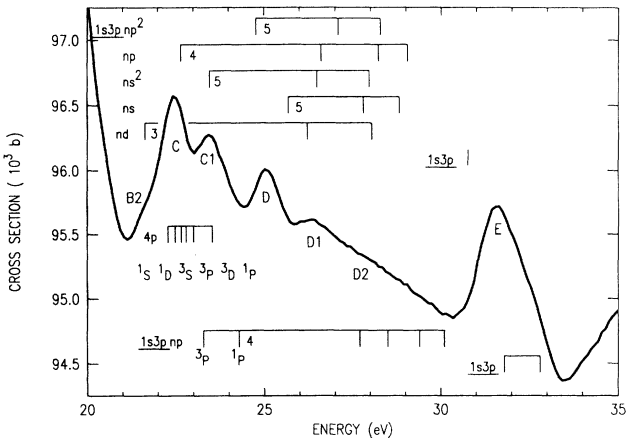

FIG. 3. Expanded view of the $1s3p$ region. Energy levels as in Fig. 2.

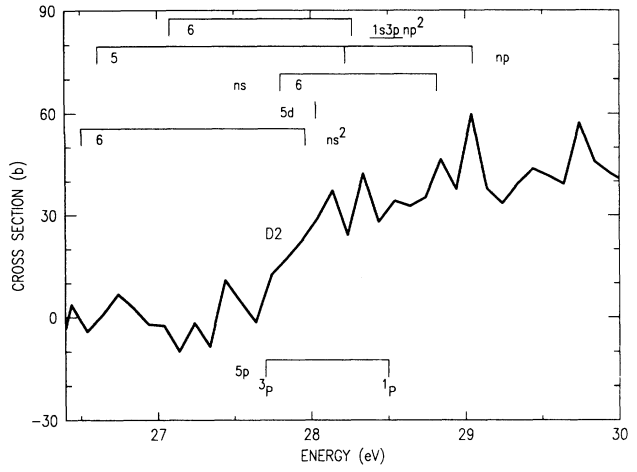

FIG. 4. The D2 feature, with a baseline subtracted. See text for discussion.

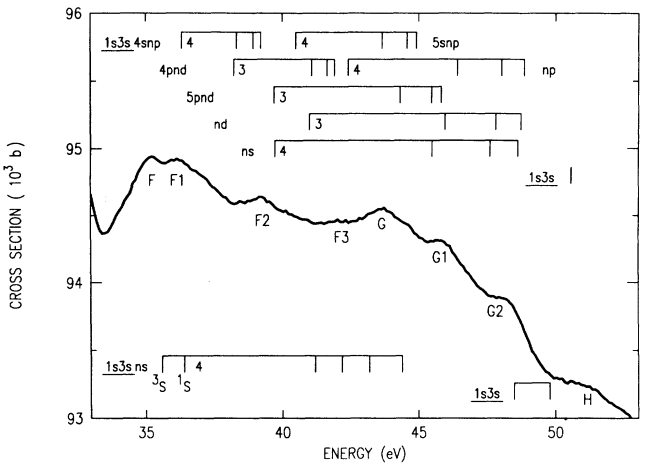

FIG. 5. Expanded view of the $1s3s$ region. Energy levels as in Fig. 2.

[9]. It also seems anomalously large compared with the 2% obtained in the same calculation for the *lower* $1s3p5p$ level. Finally, we note that a few of the newer lines seen in Fig. 2 were also resolved by Malzfeldt [14].

The strong resonance feature B, previously attributed to $1s3p4p^2$ only [2, 7], was shown by the CI calculations of Saha [5] and Cooper [6] to be dominated by $1s3p3d^2$. However, the ratio of the contributions $1s3p3d^2$: $1s3p4p^2$ is only 2:1[6]. Thus, the $1s3p4p^2$ contribution is non-negligible. Both CI [5] and SC [2, 7] calculations agree on attributing E to $1s3p4s4p$. Note that the many resonances seen in the data, in addition to features E and B, are not reproduced even by the CI calculations due to the restricted set of basis states employed, as pointed out by Saha [5].

The $1s3s$ *region.* Unlike earlier measurements [2], we were able to resolve fine structure in this region; see Fig. 5. Features F and F1 are well aligned with $1s3s(^3S,^1S)4s4p$, respectively. Note, however, that as the DF $1s3s4s$ levels [9] are lower by ~4 eV than the HF ones, an assignment to $1s3s4s$ cannot be excluded. Features F2 and the small F3 originate in the SU $1s3s4s$, $5s4p$, and the CSU $1s3s3d$, respectively, as reflected in their relative intensities. G incorporates contributions from $1s3s5snp$ ($n \geq 5$) and $1s3s4p$. G1 and G2 are due to $1s3s5s$ and $6s$ with additional contributions from nd and np levels. Furthermore, we calculate the lowest $3e$ levels $1s3p^24p(4p4d, 4s^2, 3d^2)$ to be at 40.5, 41.3, and 42.2 eV. These, and higher $3e$ levels, also contribute to G, G1, and G2, although specific $3e$ lines cannot be identified in this region. A rough comparison of the sizes of the $1s3s$ features with the $1s3p$ ones indicates a smaller cross-section ratio than the statistical 1:3 prediction of simple SC shake theory, although H is probably larger than the 1:7.5 ratio calculated by Dyall [9] for shake up. The $1s3s$ feature widths are larger by 30–50 % than the $1s3p$ ones. This points towards an enhanced Coster-Kronig depopulation of $1s3s$ levels to $1s3p$ ones as suggested earlier [2]. In view of the well-resolved $1s3s$ features measured, however, the magnitude of the enhancement may be considerably smaller than previously assumed. An accurate estimate will have to await a detailed modeling of the spectra.

The $1s3p^2$ *region.* Above the $1s3s$ edge, feature H in Fig. 5, only $3e$ features are possible. These previously unresolved features are shown in Fig. 6 with a baseline subtracted. H1, H2, and H3 are well aligned with the three major components of $1s3p^24p^2(^4P,^2D,^2S)$, as calculated by Dyall [9] and us. H4 is due mainly to $1s3p^24p$ while the very broad peak H5 contains contributions from the low-lying components of the $1s3p^2$ edge and the higher levels of the $1s3p^2np^2$, np series. While the relative cross section estimated from Fig. 6 for H1, 0.04%, is close to the 0.03% calculated by Dyall [9], his values for H2, H3, and H4 overestimate the measured ~0.1% by a factor of 2–5.

The $1s2p$ *region.* The Ar KL spectrum shown on a baseline subtracted scale in Fig. 7 was also measured

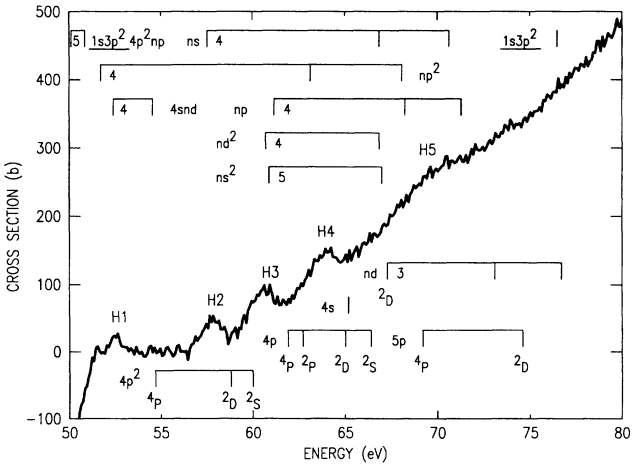

FIG. 6. Expanded view of the $3e1s3p^2$ region, with baseline subtracted. Energy levels as in Fig. 2.

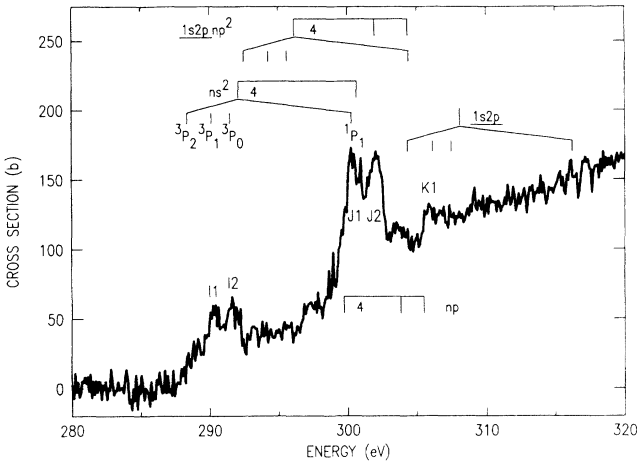

FIG. 7. Expanded view of the $1s2p$ region, with the baseline subtracted. HF energy levels are shown. Note the doublet structure of the resonance lines discussed in the text.

[15]. The resonance lines appear as doublets, the separation of which, 1.7 eV, is suggestively close to the 2.0-eV difference in the $2p_{1/2}$, $2p_{3/2}$ binding energies [16]. The spin-orbit split HF calculations suggest the following assignments. I1 and I2 are well aligned with the triplet $1s2p4p^2$ levels, while J1 and J2 are mainly due to the $1s2p4p$ ones. Alternatively, features I1 and I2 could be assigned to the triplets, and J1 and J2 to the singlets of $1s2p4p^2$ and $4p$. This assignment is supported by the equality of the calculated SOS and the measured energy difference between lines I and the J. K1 marks the onset of the $1s2p$ double-ion continuum. With $\sigma_K(300\text{ eV})=70.6$ kb and $\sigma_{J1,2}=175$ barn we obtain for J1 and J2 a relative cross section of 0.25%. As shake-up processes, unlike shake-off ones, saturate very close to threshold [17], the sudden approximation calculations of Dyall [9] are expected to hold for J1 and J2. Indeed, the measured value is in close agreement with 0.27% calculated for $2p\rightarrow np$ shake up, and slightly larger than the value of 0.2% measured for the KL edge in Kr [3]. Note, however, that as the SOS in this region is $\sim$11 eV, while the calculated average level spacing of the dominant transitions is smaller than that, additional contributions to these lines are probable.

More definitive assignments, particularly in the KL region where relaxation and exchange effects were shown to be dominant [5,6], will have to await detailed modeling of the highly resolved spectra measured in this study.

We thank C. F. Fischer for kindly supplying the interactive HF86 program. Beamtime allocation at HASYLAB and support from the Fund for Basic Research of the Israel Academy of Sciences and Humanities are gratefully acknowledged.

[1] J. M. Esteva, B. Gauthe, P. Dhez and R. C. Karnatak, J. Phys. B **16**, L263 (1983).
[2] R. D. Deslattes, R. E. LaVilla, P. L. Cowan, and A. Henins, Phys. Rev. A **27**, 923 (1983).
[3] M. Deutsch and M. Hart, Phys. Rev. Lett. **57**, 1566 (1986); Phys. Rev. A **34**, 5168 (1986).
[4] M. Deutsch and P. Kizler, Phys. Rev. A **45**, 2112 (1992).
[5] H. P. Saha, Phys. Rev. A **42**, 6507 (1990).
[6] J. W. Cooper, Phys. Rev. A **38**, 3417 (1988).
[7] K. G. Dyall and R. E. LaVilla, Phys. Rev. A **34**, 5123 (1986).
[8] J. Tulkki and T. Åberg, J. Phys. B **18**, L489 (1985).
[9] K. G. Dyall, J. Phys. B **16**, 3137 (1983).
[10] A. Krolzig, G. Materlik, A. Swars, and J. Zegenhagen, Nucl. Instrum. Methods **219**, 430 (1984).
[11] M. Breinig, M. H. Chen, G. E. Ice, F. Parente, and B. Crasemann, Phys. Rev. A **22**, 520 (1980).
[12] C. Froese Fischer, Comput. Phys. Commun. **43**, 355 (1987).
[13] S.I. Salem and A. Kumar, J. Phys. B **8**, 73 (1986) and references therein.
[14] W. Malzfeldt, Ph.D. thesis, University of Kiel, 1985 (unpublished).
[15] Related work on a similar measurement of the KL spectrum, with slightly lower resolution, was recently brought to our attention: U. Kuetgens and J. Hormes, Phys. Rev. A **44**, 264 (1991).
[16] D. A. Shirley, R. L. Martin, S. P. Kowalczyk, F. R. McFeely, and L. Ley, Phys. Rev. B **15**, 544 (1977).
[17] G. Bradley Armen, T. Åberg, K. R. Karim, J. C. Levin, B. Crasemann, G. S. Brown, M. H. Chen, and G. E. Ice, Phys. Rev. Lett. **54**, 182 (1985).